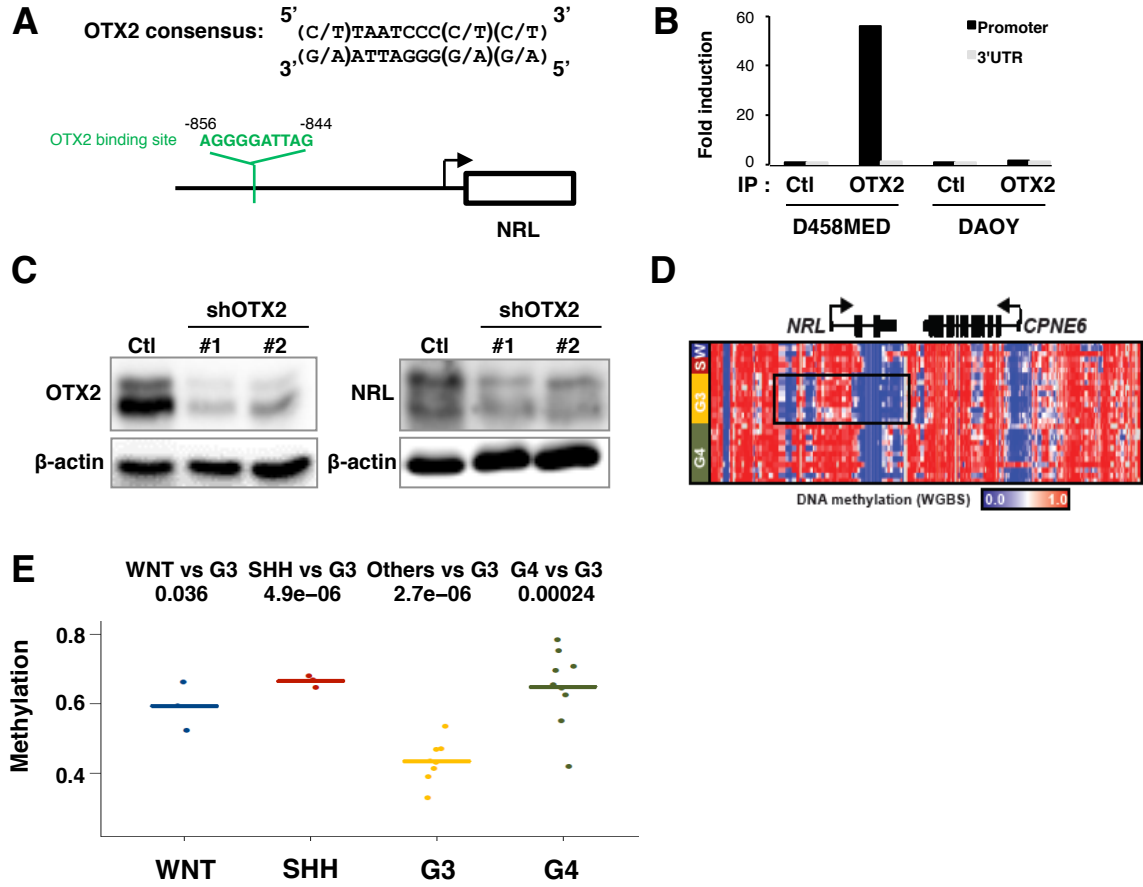


**Figure S1: NRL and CRX drive Group 3 gene expression in primary medulloblastoma. Related to Figure 1.**

(A) Enhancer rankings for the *NRL* and *CRX* adjacent super-enhancer containing region across all samples according to subgroup. (B) mRNA levels for *NRL* and *CRX* across all samples according to subgroup (same order as in A). (C) Scatter plot showing correlation of enhancer H3K27ac signal (reads per million, rpm) to mRNA level (FPKM) for *NRL* (left) and *CRX* (right). Pearson correlation statistic is provided. (D) Scatter plot showing correlation between *NRL* vs *CRX* enhancer H3K27ac signal (reads per million, rpm) (left) and mRNA level (FPKM) (right). Pearson correlation statistic is provided. (E) Scatter plot showing correlation between *OTX2* and *NRL* (left) or *CRX* (right) mRNA level (FPKM). Pearson correlation statistic is provided. (F) Boxplot showing expression of *NRL/CRX* co-target (left) or non-co-target (right) (FPKM) within super enhancer associated genes in Group 3, across MB subgroups. Boxplot center line shows data median, box limits indicate 25th and 75th percentiles, lower and upper whiskers represent 1.5x the interquartile ranges respectively. Outliers beyond the whiskers are omitted. (upper panels, G, H) Meta tracks of H3K27ac ChIP-seq signal (rpm/bp) across *NRL* & *CRX* high and low Group 3 cohorts at the *NRL* (G) locus and the *CRX* (H) locus. (lower panels) Heatmap of DNA methylation for each sample is shown below with hypomethylated regions boxed. (I) Scatter plot showing correlation between *NRL* (left) or *CRX* (right) mRNA level (FPKM) and +/- 5kb TSS DNA methylation (WGBS). Pearson correlation statistic is provided. (J) Top: waterfall plot showing Group 3 active genes (x-axis) ranked by the average log<sub>2</sub> fold change in enhancer and promoter H3K27ac load (y-axis) between *NRL* & *CRX* high vs. low tumors (n of 4 each). Middle: average binned log<sub>2</sub> gene expression fold changes for genes ranked as above. Active genes were evenly distributed across 100 bins. Error bars represent that 95% confidence intervals of the mean for each bin as determined by empirical resampling. Bottom: leading edge enrichment of *NRL/CRX* co-target genes across active genes as ranked above.



**Figure S2: OTX2 regulates NRL expression in Group 3 MB by binding to its hypomethylated promoter. Related to Figure 1.**

(A) Schematic representation of the human *NRL* promoter. A potential OTX2 binding site is indicated. Note that the potential OTX2 binding site in the *NRL* promoter matches its consensus. (B) Chromatin Immunoprecipitation (ChIP) analysis of OTX2 binding to the *NRL* promoter. qPCR was performed to quantify the enrichment of the OTX2 binding site within the *NRL* promoter following immunoprecipitation with the OTX2 antibody (IP OTX2) or a control antibody (IP Ctl) in D458MED. DAOY cells that do not express *NRL* were used as negative control. (C) Expression level of OTX2 (left) and NRL (right) by immunoblot in D458MED following downregulation of OTX2 by shRNA (shOTX2#1 and #2) relative to control shRNA (Ctl).  $\beta$ -actin was used as a loading control. (D) Whole genome bisulphite sequencing (WGBS) data showing DNA methylation tracks for primary MB samples at the *NRL* locus. Hypomethylated regions overlapping the *NRL* promoter in Group 3 are demarcated with a box. (E) Summary of DNA methylation levels detected within +/-5kb of the *NRL* promoter across MB subgroups. p-values are indicated. The center line shows data median, dots represents level of methylation in each tumor.

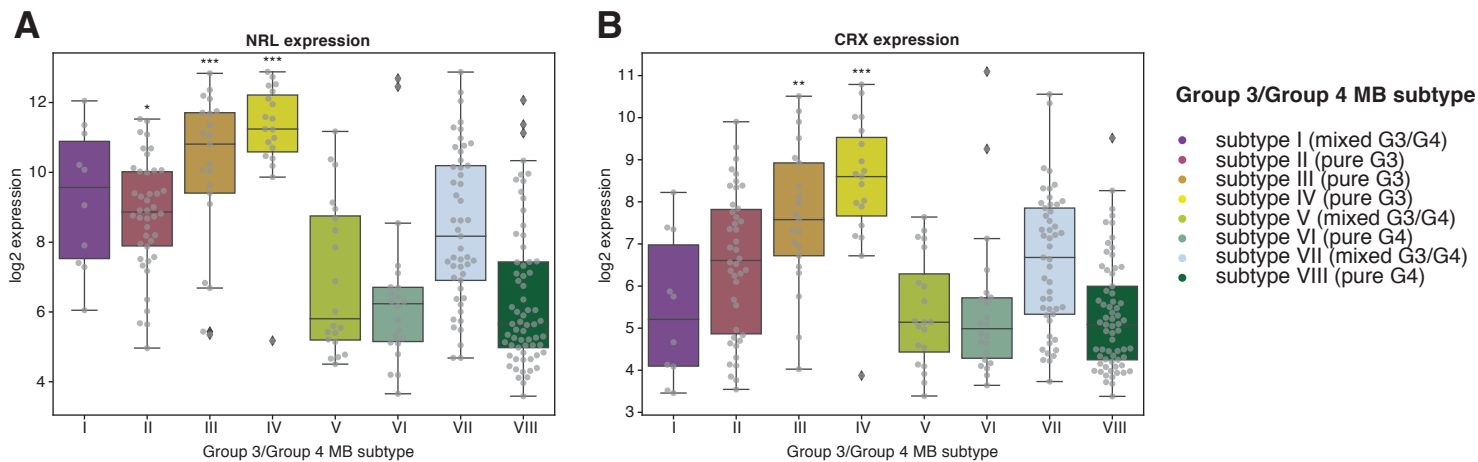


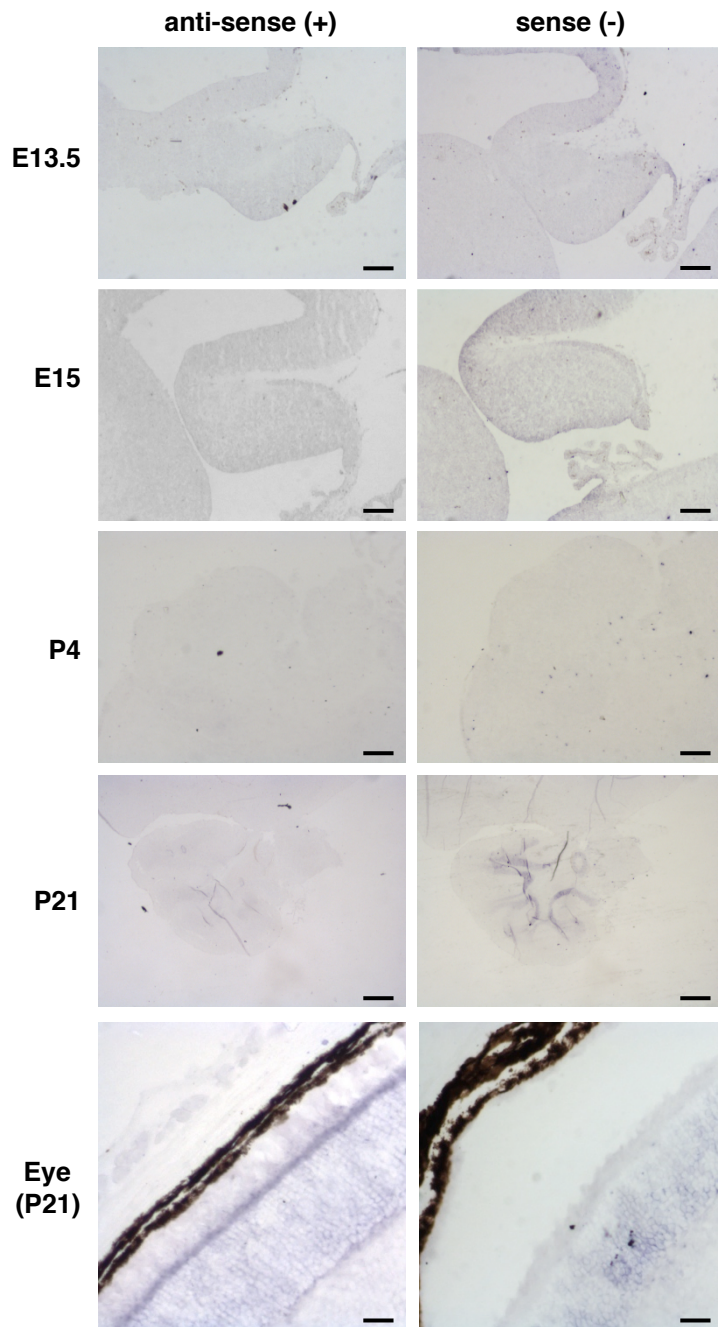
**Figure S3: Expression of NRL and CRX in Group 3/Group 4 MB subtypes. Related to Figure 1.**

(A, B) Boxplots summarizing NRL (A) and CRX (B) expression in the context of recently described Group 3/Group 4 MB subtypes (n=248 samples profiled by Affymetrix expression array; Northcott et al, 2017). Significance was determined using a one-sided Mann-Whitney U test for each subtype vs. the rest and p-values corrected by accounting for the FDR (False Discovery Rate). \* $P < 0.05$ , \*\* $P < 0.0005$ . Description of Group 3/Group 4 MB subtypes is indicated. Boxplot center lines show data median; box limits indicate the 25th and 75th percentiles; Upper whiskers indicate 1.5x the interquartile range (IQR) more than the third quartile; Lower whiskers indicate 1.5x IQR lower than the first quartile; Outliers are represented by individual diamonds outside upper and lower whiskers; Individual points represent individual samples.

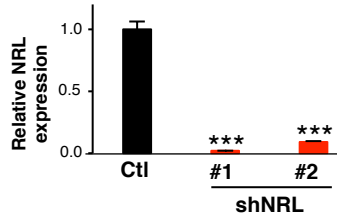
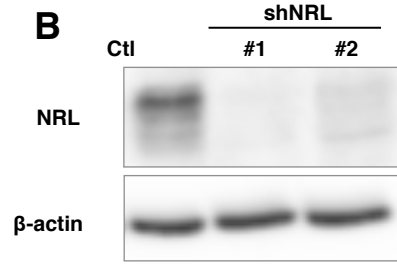
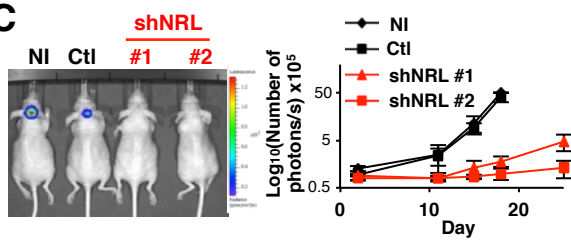
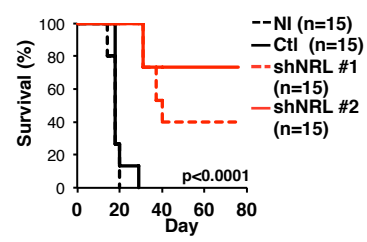
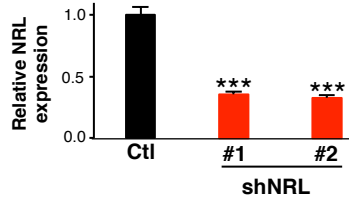
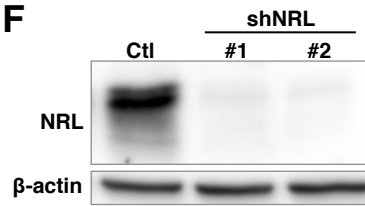
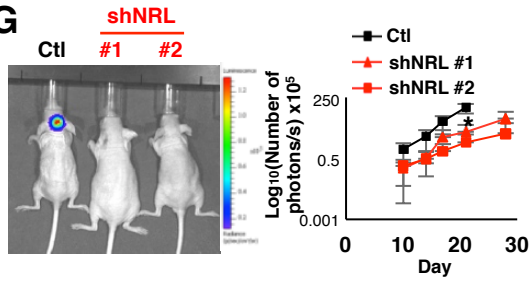
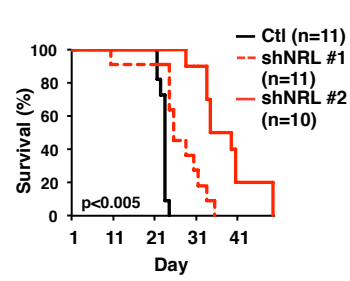
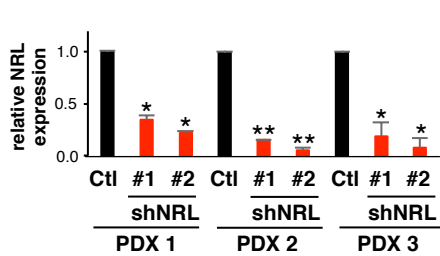
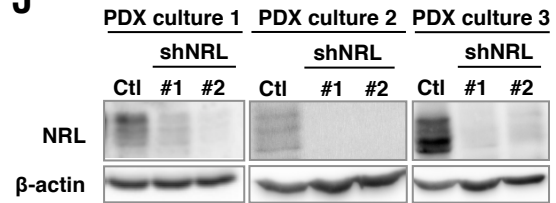
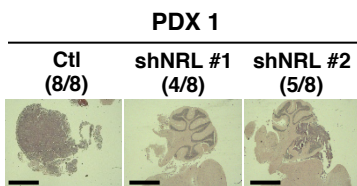
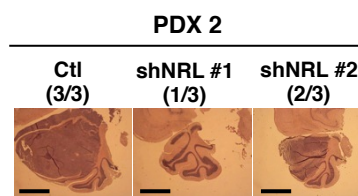
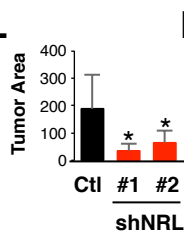
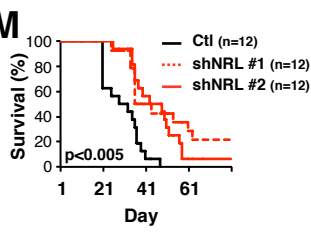
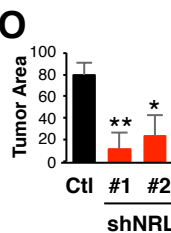
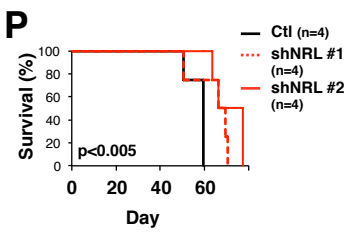
\* indicates False Discovery Rate (FDR) corrected Mann-whitney U test p-value  $\leq 0.05$ ;

\*\* indicates FDR corrected Mann-whitney U test p-value  $< 0.005$ ,

\*\*\* indicates FDR corrected Mann-whitney U test p-value  $< 0.0005$ .



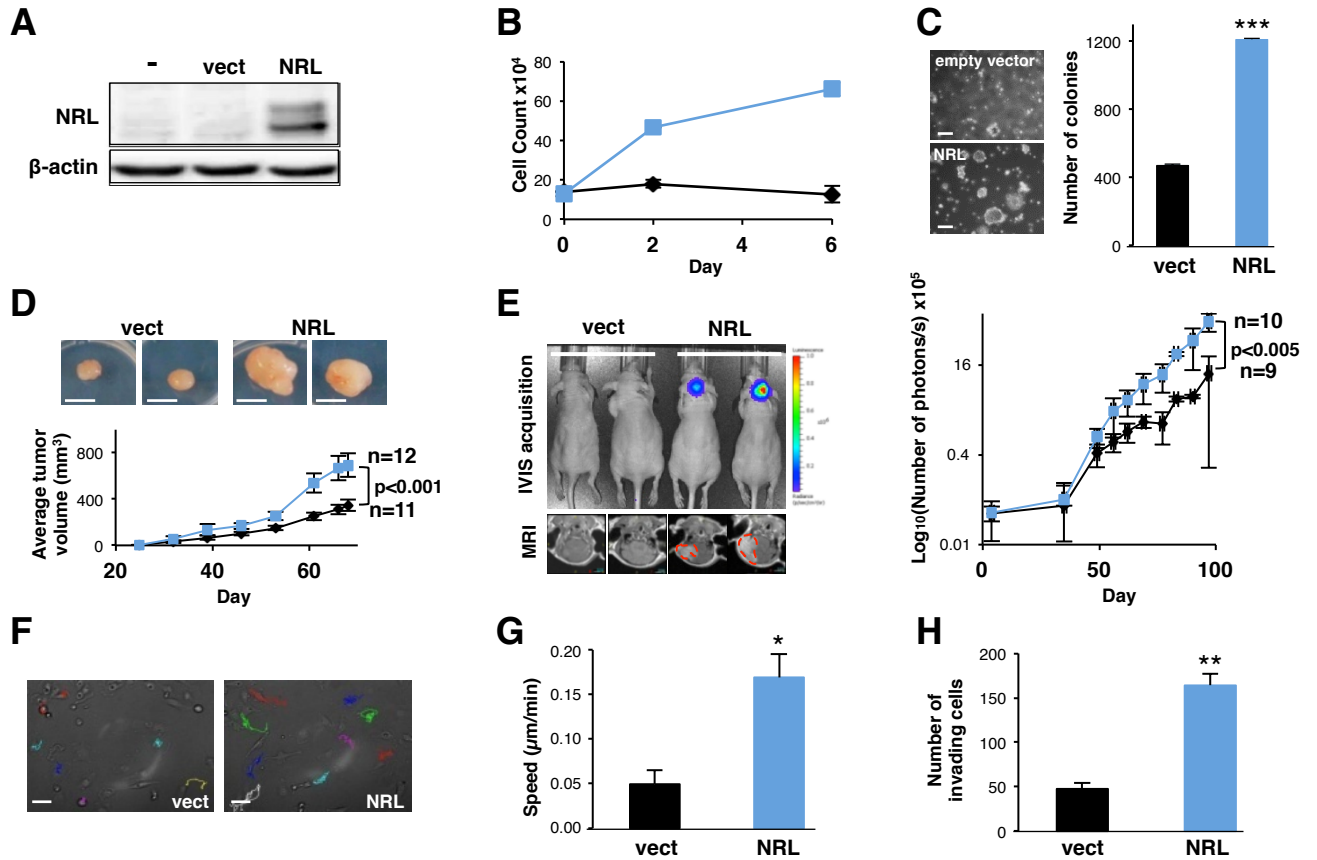
**Figure S4: Absence of *NRL* expression during mouse cerebellum development. Related to Figure 1.** In situ hybridization (ISH) was performed at different embryonic (E13.5, E15) or postnatal (P4, P21) stages of the mouse cerebellum development. Antisense *NRL* probe was hybridized and sense probe was used as a negative control. As a positive control, ISH was performed on mouse retina at stage P21. Note the signal on the photoreceptor layer in the retina. Scale bars, 125 $\mu$ m (E13.5, E15, P4), 500 $\mu$ m (P21) and 25 $\mu$ m (Eye, P21) .

**A****B****C****D****E****F****G****H****I****J****K****N****L****M****O****P**

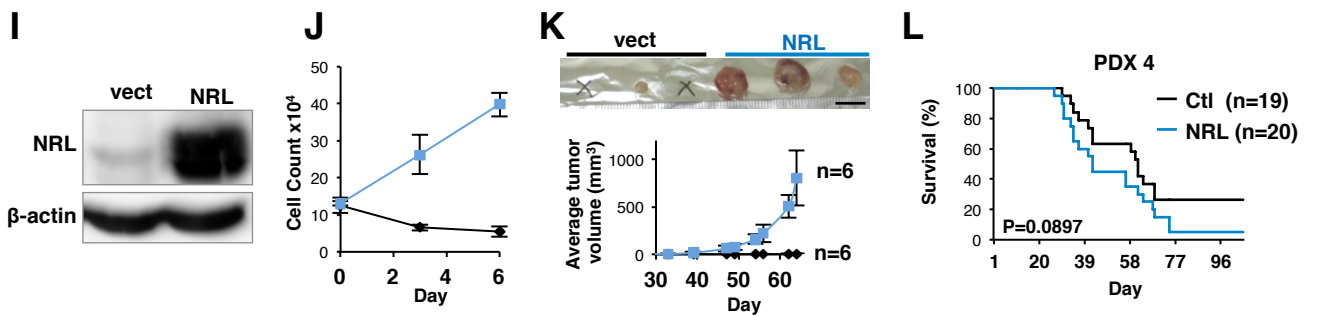
**Figure S5: Knockdown of NRL decreases MB growth and increases survival *in vivo*. Related to Figure 2.**

Effect of shRNA-mediated NRL down-regulation in two cell lines, D458MED (A-D) and HDMB03 (E-H). (A and E) RT-qPCR on RNA extracted from D458MED (A) or HDMB03 (E) cells infected by lentivirus encoding control shRNA (Ctl, black bar) or targeting NRL (red bars). (B and F) Immunoblot analysis of NRL in control and knockdown cells as indicated. (C-D and G-H) Effect of shRNA-mediated NRL down-regulation in the D458MED (C-D) and HDMB03 (G-H). (C-D and G-H) Control and knockdown D458MED and HDMB03 cells were orthotopically grafted into the cerebellum of NUDE mice. (C and G) Tumor growth was assessed by bioluminescence using IVIS imaging. An image of luciferase signal on representative animals is shown. (right panel). (D-H) Kaplan Meier survival curves of these mice (NI: not infected (black dashes), Ctl: shRNA control (black line), shNRL#1 (red dashes), shNRL #2 (red line)). The number of mice per group is indicated. \*\*\*p-value<0.0001. Panels A, B, D are identical to panels E, F (left) and G of main Figure 2.

(I-P) Effect of shRNA-mediated NRL down-regulation in 3 PDXs (PDX1, PDX2, PDX3). (I) Relative expression of *NRL* by RT-qPCR on RNA extracted from PDX cells infected by lentivirus encoding control shRNA (Ctl, black bar) or targeting NRL (red bars). (J) Immunoblot analysis of NRL in control and knockdown cells as indicated. (K-P) Effect of shRNA-mediated NRL down-regulation in the PDX1 (K-M) and PDX2 (N-P). Control and knockdown PDX1 (K-M) and PDX2 (N-P). Cells were orthotopically grafted into the cerebellum of NUDE mice. Mice were monitored weekly and the entire cohort was sacrificed when the first MB symptoms were detected in the first animal. (K, N) MB was verified by Hematoxylin and Eosin (H&E) staining on sections. The tumor incidence for both PDXs is indicated on the top. Scale bars, 600 $\mu$ m. (L, O) Quantification of tumor area using Image J software. (M, P) Kaplan Meier survival curves of mice transplanted with PDX1 (M) and PDX2 (P) (Ctl: shRNA control (black line), shNRL#1 (red dashes), shNRL#2 (red line))., The number of mice per group is indicated. \*p-value<0.01, \*\*p-value<0.001. Panels J (left: PDX culture 1) and M are identical to panels F (right) and H of the main Figure 2. The p value was determined by unpaired t test for qPCR analysis. The p value for survival was determined by log-rank (Mantel-Cox) test for each Kaplan Meier survival curves. Error bars represent the mean  $\pm$  SD.



**DAOY**



**ONS-76**

**PDX 4**



**Figure S6: NRL overexpression increases medulloblastoma growth. Related to Figure 2.**

(A-H) NRL overexpression increases the transformed phenotype of the DAOY MB cell line. DAOY were stably transfected with a control vector alone (vect, in black) or with an NRL-encoding vector (NRL, in blue). (A) Western blot analysis of ectopic NRL expression in transfected DAOY cells. The parental DAOY is shown (-). (B) Growth curve on DAOY cultures stably expressing or not *NRL* in low serum condition (0.2% FCS). (C) Anchorage independent growth of the different DAOY cultures assessed by colony formation in soft agar. Representative photographs (left) and quantification (right). Scale bar, 150 $\mu$ m. (D) The different cultures were grafted subcutaneously in nude mice and tumor growth was followed. Representative tumors are shown on the top (Scale bar, 5mm) and the average of tumor size is shown on the bottom. Mice were grafted with NRL-expressing DAOY (n=12) and with control cells (n=11). (E) DAOY cells stably expressing the luciferase gene were generated to monitor tumor growth by bioluminescence (IVIS). Images of two representative mice from each group at the end of the experiment are shown on the left (bioluminescence signal on the top and MRI signal on the bottom). The average of the light signal for each group (n=9 vect in black and n=10 NRL in Blue) during the course of the experiments is represented on the right. (F-G) Migration of the DAOY cultures was tracked by videomicroscopy. (F) A representative field showing the path of the individual cells during the course of the experiment is presented (Scale bar, 5 $\mu$ m) and (G) the average speed ( $\mu$ m/min) quantified. (H) DAOY cultures were seeded on matrigel invasion chamber and their ability to migrate through the matrigel was quantified. \*p-value<0.01, \*\*p-value<0.001 and \*\*\*p-value<0.0001.

(I-K) NRL overexpression increases the transformed phenotype of the ONS-76 MB cell line. ONS-76 cells were stably transfected by control vector alone (-, in black) or by NRL encoding vector (NRL, in blue). PDX4 cells were infected with lentivirus control (ctl) or encoding for NRL (blue). (I) Immunoblot showing the ectopic NRL expression in ONS-76. (J) NRL overexpression increases ONS-76 cell proliferation in low serum conditions (0.2% FCS) *in vitro*. Growth curve was obtained by counting cells at regular intervals. (K) Ectopic NRL expression increased ONS-76 tumorigenicity upon subcutaneous injection (n=6 for each group). Cells were injected in the right flank of the mouse and tumor growth was determined by measuring tumor size. Photographs of representative tumors are shown (top; scale bar, 1cm) and tumor volume over time is represented on the graph (bottom).

(L) NRL overexpression increases the transformed phenotype of MB PDX. PDX4 control cells (Ctl) or expressing NRL (blue line) were orthotopically transplanted into Nude mice. Kaplan Meier survival curves of these mice. The number of mice per group is indicated. The p value was determined by unpaired t test. Error bars represent the mean  $\pm$  SD.

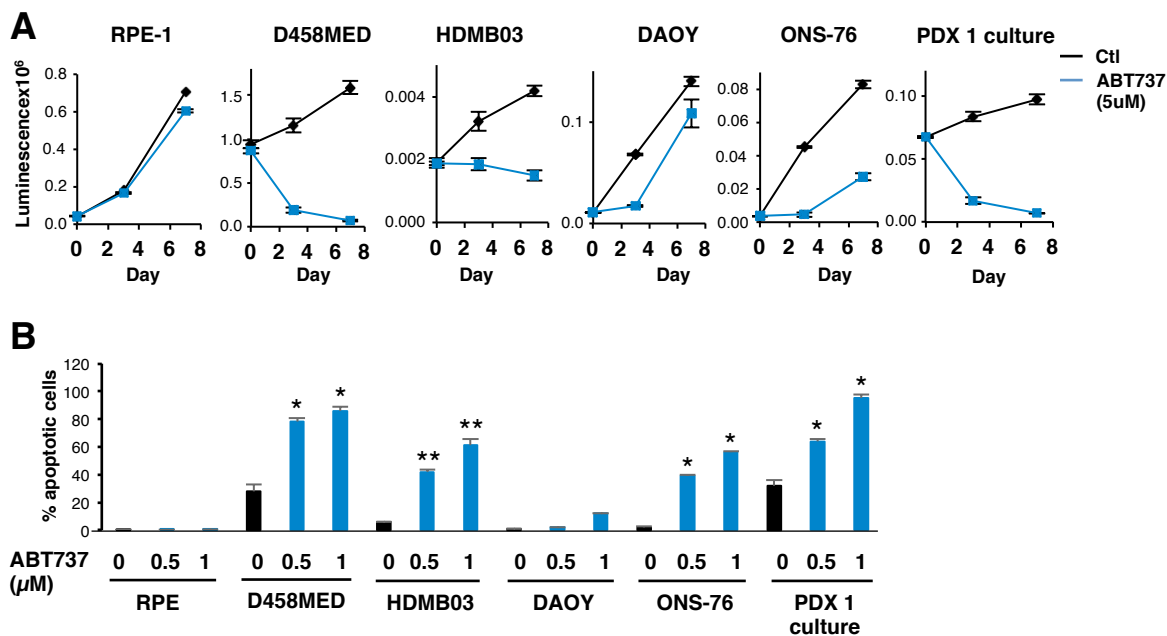


**Figure S7: The BCL inhibitor ABT737 affects MB growth *in vitro*. Related to Figure 8.**

The effect of ABT737 (shown in blue) was compared to vehicle (Ctl, in black) on different models *in vitro*. (A) Cell viability was measured *in vitro* by luminescence using Cell titer Glo assay in control or in ABT737 treated cells as indicated (RPE-1, D458MED, HDMB03, DAOY, ONS-76, PDX1). Cells were treated every 2 days with 5 $\mu$ M of ABT737. (B) Apoptosis was assessed by measuring cleaved caspase 3 levels by FACS 48h after seeding in control condition (ctl) or upon ABT737 treatment (0.5 and 1 $\mu$ M).